Jisha Joseph "Self-assembly of structurally diverse phosphomolybdates: synthesis, structure and properties." Thesis. Research and Post gradute Department of Chemistry, St. Thomas college (autonomous), University of Calicut, 2020.

CHAPTER V

Removal of cationic dyes from water using APM
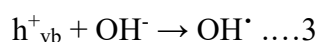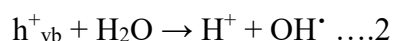
Summary

Micro-sized spherical ammonium phosphomolybdate (APM) particles were synthesized under ambient conditions. The composition and morphology of APM was established by powder X-ray diffraction, energy dispersive X-ray analysis, fourier transform infrared spectroscopy, thermogravimetric analysis and scanning electron microscopy. Further, the ability of APM particles to remove dye from dye-contaminated water was monitored with respect to nature of incident radiation, concentration, pH and nature of dye. APM could effectively remove cationic dyes from water as long as the pH range permitted the dye to retain its cationic behavior. The results suggested that the removal of dye-stuffs could be attributed to ion-exchange between ammonium ions in APM with cationic dye moieties. APM could be reused several times without affecting its efficiency. Removal efficiency of 94.6% could be retained upto 16th cycle and sensitivity to pH enabled APM to reverse the cation exchange process. The ion-exchange process was not dependent on exposure of APM particles to irradiation which confirmed that the mode of action of APM was not photocatalytic in nature.

V.1. Introduction

Rapid industrialization and increase in population density has resulted in severe contamination of water resources [1]. In particular, water pollution caused by dyes has become a serious threat due to its high toxicity and stability to resist degradation even under extreme conditions [2,3]. Extensive research over the past decades has resulted in various dye removal techniques that depend on physical, chemical and biological processes [4-8]. Among these, the techniques that rely on adsorption of dyes have a major advantage over other techniques that rely on degradation of dyes because potentially hazardous secondary metabolites can also be generated during degradation of dyes [9]. Conventionally adsorbents such as activated carbon [10], bio-waste [11], zeolites [12] and clay materials [13] have been used to treat dye-contaminated water but they suffer from low adsorption capacity and poor selectivity. Therefore, there has been a constant effort in developing new materials that can effectively remove dye moieties from water.

For the past few years, researchers have been involved in the synthesis of porous and functionalized phosphomolybdate (PMO) cluster based solids [14-17]. Owing to structural features such large surface area, porosity, tuneable shape and size; these solids have been explored for potential applications in areas of catalysis [18-20], electrical conductivity [21], luminescence [22-25], magnetism [26-27], non-linear optics [28] and as anti-tumour agents [29,30]. Among these, ammonium phosphomolybdate (APM), $\{NH_4\}_3[PMo_{12}O_{40}].xH_2O$ is a versatile PMO cluster based solid which was first synthesized by Berzelius in 1826 [31]. Although it has been used as electrode material, catalyst and adsorbent [32-34]; the ion-exchange behavior of APM for the removal of dye-stuffs from water has not been reported so far. However, in literature there are few
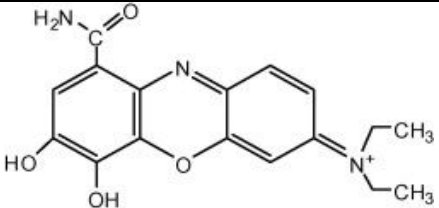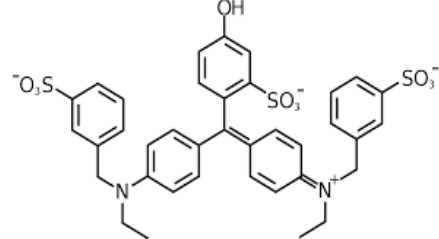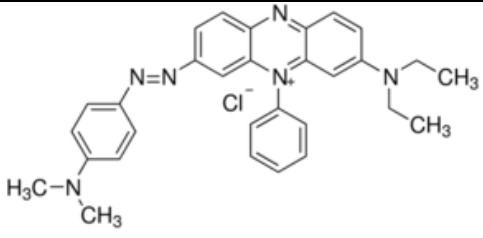
examples wherein it has been reported as a photocatalyst for the degradation of selected dye stuffs (Table V.1). It was reported that degradation was brought about by the photo excitation of the metal oxides, followed by the formation of electron–hole pair on its surface. The reactive intermediate which was responsible for the degradation of dye was hydroxyl radical (OH$^•$). It was either formed by the decomposition of water or by the reaction of hole with OH$^-$ (available in form of base that is added to the reaction medium). Subsequently, the hydroxyl radical resulted in partial or complete degradation of dyes.

$$APM + h\nu \rightarrow APM\ (e^-_{cb} + h^+_{vb})\ ....1$$

$$h^+_{vb} + H_2O \rightarrow H^+ + OH^•\ ....2$$

$$h^+_{vb} + OH^- \rightarrow OH^•\ ....3$$

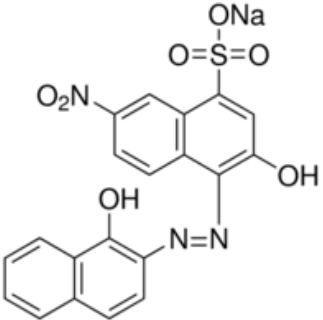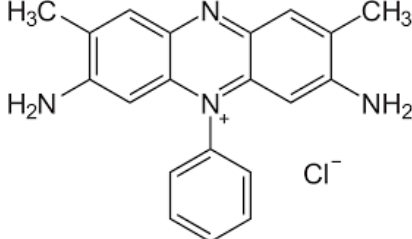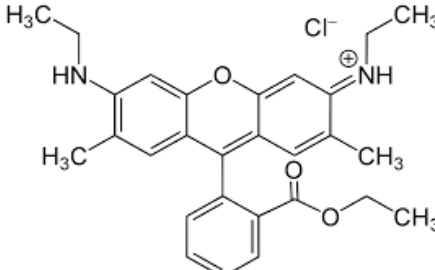$$OH^• + Dye \rightarrow Degradation\ of\ the\ dye\ ....4$$

The mechanism for degradation of dyes and the results obtained have been summarized in Table V.1. Most of the results reported in literature with APM suggested that photo excitation of APM followed by absorption of OH$^•$ radical in holes was responsible for the degradation of dyes (referred to as Mechanism **V.1** in Table V.1).

Based on the above considerations, in this chapter four dyes *viz.* Methylene Blue, Eosin Y, Malachite Green and Methyl Red were selected and their solution was treated with APM. The decolorization of dye-stuffs was recorded with respect to the change in intensity of absorption peaks using UV-Visible spectroscopy. Effect of variables such as nature, concentration and pH of dye-stuffs was further investigated and a plausible mechanism for the action of APM on dye-stuffs has been proposed.

Table V.1. Table summarizing the results obtained using APM for degradation of dye-stuffs.

Sl. No.	Dye	Structure	Nature of dye	Mechanism for degradation	Time taken for complete degradation	Reference
1.	Celestine blue B		Cationic dye	Photo excitation of the APM followed by absorption of OH radical in holes. Maximum degradation was observed in basic medium	97.7 % degradation in 4 hours	35
2.	Fast Green		Behaves as anionic dye above pH-6	The rate of photocatalytic bleaching of dye increases with increases in pH till 6.0 according to Mechanism **V.1**. Above pH 6 the anionic dye will face a force of repulsion from negatively charged surface of the dye which prevents the degradation	Not reported	36
3.	Janus Green B		Basic azo and cationic dye	The rate of photocatalytic degradation of Janus Green B increases with increase in pH (upto pH = 11) according to Mechanism **V.1**. Above pH 11, the approach of electron rich dye to the semiconductor surface is retarded which resulted in a decrease in the rate of photocatalytic degradation of dye	Color removal of 97.9% was achieved in 4 hours	37

4.	Eriochrome Black-T		Azodye	Under acidic conditions, dye was not degraded but in the basic range, the dye solution was degraded according to Mechanism **V.1**. The rate of photocatalytic degradation increases with increase in pH (upto pH = 11) Above pH 11, a decrease in the rate of photocatalytic degradation of dye was observed	Maximum degradation of 93.9 % was achieved after irradiation time of 5 hours	38
5	Safranin O dye		Heterocyclic azine dye	The degredation of safranin O on irradiation with visible light follow pseudo first order kinetics	96.8% of safranine O dye was degraded with the addition of 4g/L of APM	39
6	Rhodamine-6G		Cationic dye	Upto pH 9.0, the rate of photodegradation of dye increases with increase in pH (Mechanism **V.1**). However, above pH 9.0, decrease in the rate of photodegradation was observed	Not reported	40

V.2. Experimental Section

V.2.1. Synthesis of APM

All reagents were of reagent grade and were used as received from commercial sources without further purification. Initially, two solutions were prepared. Solution A was prepared by mixing 11.05 g of ammonium heptamolybdate, $(NH_4)_6Mo_7O_{24}.4H_2O$ with 15 ml of ammonia solution and 10 ml of distilled water. The solution was boiled and made upto 250 ml. Secondly, 40 ml of 0.067 M solution of $Na_2HPO_4 \cdot 12H_2O$ (disodium hydrogen phosphate dodecahydrate) was mixed with 20 ml of conc. HNO_3 and was labelled as solution B. Subsequently 100 ml of Solution A was added to Solution B and stirred for 10 minutes. The resultant solution was kept undisturbed for 18 hours and the precipitate formed was allowed to settle down. Finally, it was filtered and the canary yellow precipitate of APM thus obtained was washed with water and air-dried.

V.2.2. Synthesis of dye solutions

10^{-4} M stock solutions of Methylene Blue (MB), Eosin Y (EY), Malachite Green (MG) and Methyl Red (MR) were prepared by dissolving definite amount of dye in distilled water. The stock solutions were further diluted to 10^{-5} M for the present study.

V.2.3. Treatment of dye-contaminated water

MB, EY, MG and MR show absorbance peak between 650-700 nm, 500-550 nm, 600-650 nm and 500-550 nm respectively [41-44]. Initially, 25 ml of 10^{-5} M MB solution was taken and its pH was adjusted to 5.0±0.1 using 1M HCl. Subsequently, 0.125 g of APM was added

to it and the mixture was kept under stirring for 5 minutes. Thereafter, it was left undisturbed for 1 hour. Finally, the MB solution was centrifuged and the filtrate was analyzed using UV-Visible spectroscopy. The absence of absorbance peak at $\lambda_{max} = 660$ nm indicated that MB had been removed from the solution. Based on the result obtained (discussed later), the effect of various factors such as contact time, pH, nature of dye and amount of APM was further investigated.

The removal of dye-stuffs was monitored with respect to change in the intensity of the absorbance peaks using UV-Visible spectroscopy (Shimadzu UV-Visible 1800 double beam spectrophotometer).

The dye removal efficiency of APM was calculated by

$$\text{Removal efficiency (\%)} = \frac{(C_i - C_f)}{C_i} \times 100$$

where, C_i and C_f concentration of dye before and after the treatment with APM [45].

V.3. Characterization

Fourier transform infrared (FTIR) spectrum was recorded on KBr pellets using Shimadzu FTIR spectrophotometer (model: IR Affinity). Before recording the FTIR spectrum, the sample was heated at 120°C for 1 hour. Thermogravimetric analysis (TGA) was done on Perkin-Elmer TGA7 from room temperature to 700°C at a heating rate of 10°C/min in nitrogen atmosphere to determine water content and overall thermal stability of the product. Scanning electron microscopic studies (SEM) were carried out on as-synthesized APM powder mounted on carbon tape using FEI FESEM Quanta 200 at an accelerating voltage of 10 kV. Powder X-ray diffraction (PXRD) data was collected on a Malvern Panalytical Aeris

diffractometer using Ni-filtered Cu Kα radiation. Data was collected with a step size of 0.02° and count time of 2 s per step over the range 5° < 2θ < 60°. Nitrogen adsorption and desorption (BELSORP-mini II machine, BEL Japan Inc., Japan) was employed to characterize and measure the pore volume. Before the nitrogen adsorption-desorption measurement, the sample was thoroughly dried at 150°C under vacuum for two hours.

V.4. Results and discussion

V.4.1. Characterization of APM particles

The PXRD pattern of APM particles was found to match well with JCPDS file no. 43-0315 indicating the formation of single-phasic cubic {NH$_4$}$_3$[PMo$_{12}$O$_{40}$].xH$_2$O having lattice constant a = 11.67 Å (Figure V.1a). FTIR spectrum showed the presence of bands in the region 1100-700 cm^{-1} which are characteristic of Keggin type heteropoly anions [46]. The spectrum also showed four FTIR bands at 1067, 964, 869 and 788 cm^{-1} that could be attributed to P-O and Mo-O stretching respectively. Bands at 3212 and 1606 cm^{-1} were assigned as N-H stretching and N-H bending respectively due to the absorption of NH$_4^+$ ions [47].

The morphology and dimension of APM particles was characterized by SEM. SEM image of APM showed the formation of agglomerated particles having plane faces with diameter 4.5-9 μm (Figure V.1b). Figure V.1c shows the TGA thermogram obtained by heating as-synthesized APM, {NH$_4$}$_3$[PMo$_{12}$O$_{40}$].xH$_2$O at 10°C/min from room temperature to 700°C. Two weight loss steps were observed. The initial weight loss of ~5.4% upto 120°C could be attributed to the dehydration of the as-synthesized APM, {NH$_4$}$_3$[PMo$_{12}$O$_{40}$].xH$_2$O wherein

x was found to be 6. The value was in good agreement with theoretical value (5.44%) for weight loss corresponding to six molecules of water of crystallization.

$${NH_4}_3[PMo_{12}O_{40}].6H_2O \rightarrow {NH_4}_3[PMo_{12}O_{40}] + 6H_2O \dots (5)$$

The second weight loss of ~4.1% between 120-500°C indicated the decomposition of the Keggin anion and the evolution of constitutional water together with ammonia gas according to

$${NH_4}_3[PMo_{12}O_{40}] \rightarrow 3NH_3 + 3/2\ H_2O + \tfrac{1}{2}\ P_2O_5 + 12\ MoO_3 \dots (6)$$
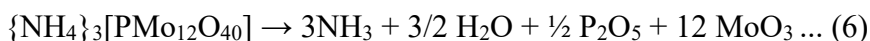
The second weight loss (4.1%) was also found to be in good agreement with the theoretical value (4.15%) and the values reported earlier in literature [48-49].
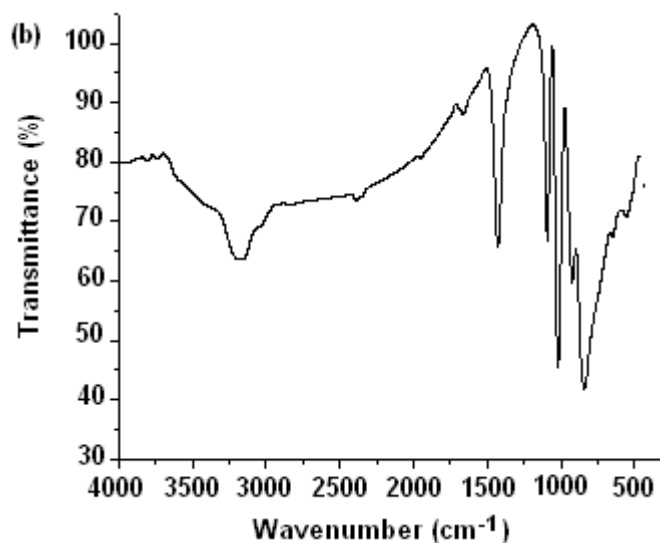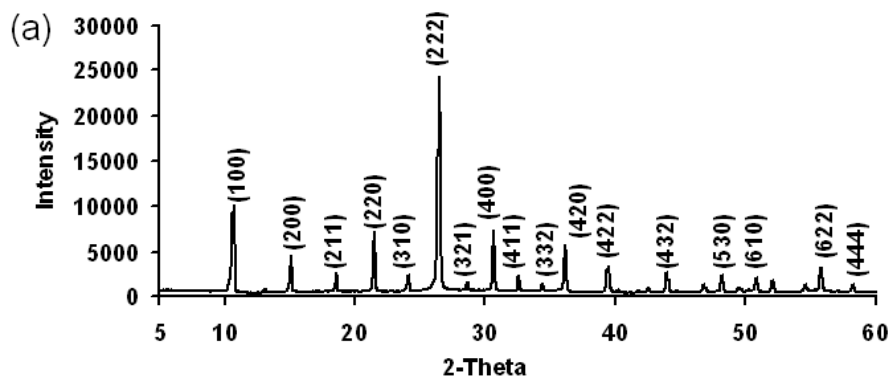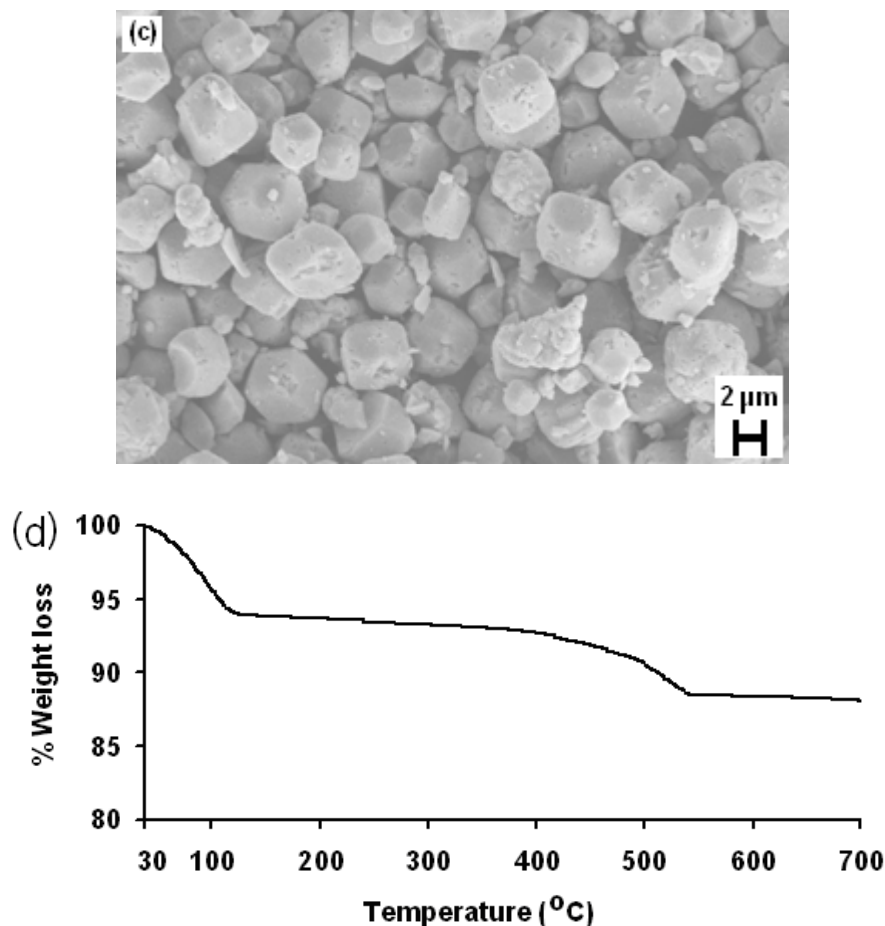
Figure V.1. (a) Indexed PXRD pattern (b) FTIR spectrum (c) SEM image and (d) TGA curve of as-synthesized APM particles.

V.4.2. Treatment of dye contaminated water

V.4.2.1. Effect of nature of light

Initially, 25 ml of 10^{-5} M Methylene Blue (MB) dye solution having pH = 5.0±0.1 was taken in three beakers. 0.125 g of APM was added to each of the beakers; the solutions were stirred for 5 minutes and kept undisturbed for 1 hour under the following conditions:

I) The first beaker was kept in dark.

II) The second beaker was kept in sunlight.

III) The third beaker was kept under UV light.

The above solutions were centrifuged after 1 hour and filtered. The filtrate was analyzed using UV-Visible spectroscopy. The absence of absorbance peak at $\lambda_{max} = 660$ nm indicated that MB had been removed from each of the beakers (Figure V.2, also refer Table V.2). The maximum dye removal efficiency of APM was found to be 94.6%. It was also observed that the colour of APM collected from beakers kept in dark, sunlight and UV light had changed from yellow to green after treatment with MB solution. A comparison of PXRD pattern of APM before and after treatment with MB solution confirmed that there were no structural changes in APM upon treatment with MB (Figure V.3). The above experiment also indicated that the mode of action of APM was not photocatalytic in nature.

Table V.2. Absorbance of MB solution upon treatment with APM at 660 nm after 1 hour of irradiation under different conditions.

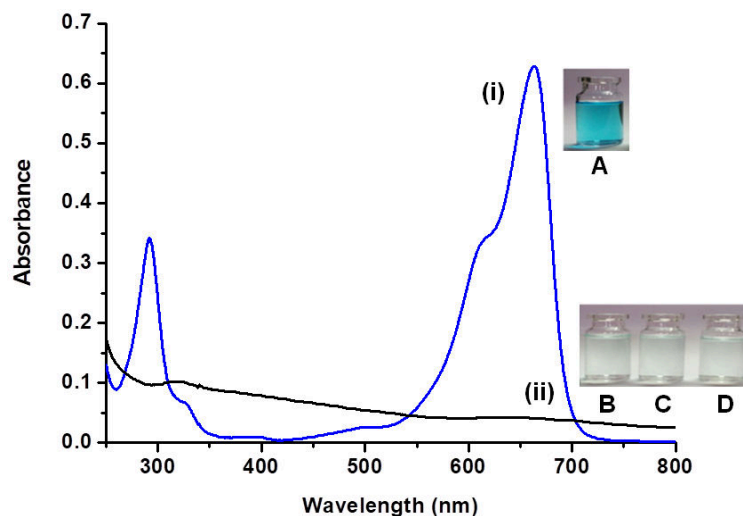| Bottle	Type of irradiation	Absorbance
A	Initial MB solution	0.65
B	Dark	0.042
C	Sunlight	0.041
D	UV light	0.041

Figure V.2. Figure showing UV-Vis spectra of (i) original solution of Methylene Blue (MB) having pH = 5.0±0.1 and (ii) MB solution obtained after treatment with APM followed by exposure to dark, sun light and UV for 1 hour. Figures in the inset represent the original solution of MB (Bottle A) and filtrate of Bottle A obtained after treatment with APM followed by exposure to dark, sun light or UV for 1 hour (Bottle B-D) respectively.
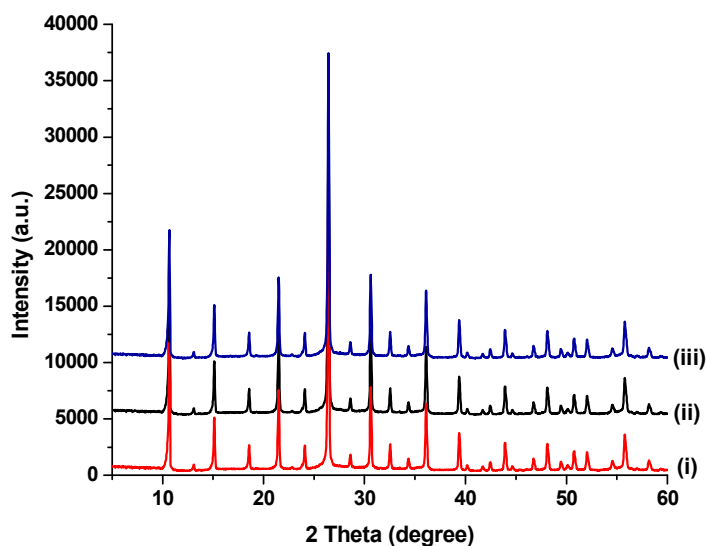

Figure V.3. Figure showing PXRD of APM collected from (i) Bottle B (ii) Bottle C and (iii) Bottle D.

V.4.2.2. Effect of contact time

25 ml of 10^{-5} M MB dye solution having pH = 5.0±0.1 was taken in five beakers. 0.125 g of APM was added to each of the beakers and the solutions were stirred for 5 minutes. The solutions were left undisturbed and centrifuged after different time intervals (0, 15, 30, 45 and 60 minutes). Subsequently, the filtrate from each beaker was monitored using UV-Visible spectroscopy Figure V.4. From Figure V.4 it is evident that the removal of MB (removal efficiency = 94.6%) takes place instantaneously i.e. as soon as the dye comes in contact with APM (also refer Table V.3).
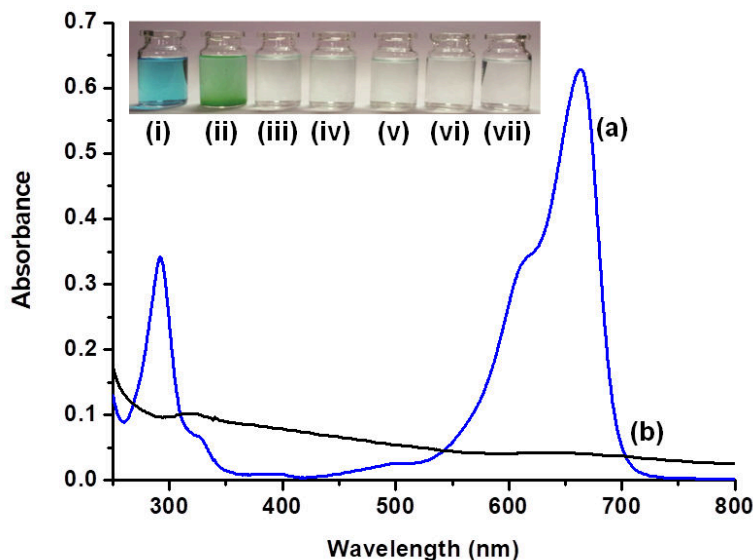

Figure V.4. Figure in the inset shows the results obtained for time bound decolourization of MB (pH = 5.0±0.1).

(i) Original dye solution

(ii) Dye solution immediately after adding APM.

(iii) - (vii) Filtrate collected after 0, 15, 30, 45 and 60 minutes respectively.

(a) and (b) Represent the corresponding UV-Visible spectra of original MB solution i.e. Bottle (i) and filtrate of Bottles (iii-vii) respectively.

Table V.3. Absorbance of MB solution upon treatment with APM at 660 nm upon varying time of contact.

Bottle	Time of contact (minutes)	Absorbance
(i)	Not applicable	0.650
(iii)	0	0.041
(iv)	15	0.040
(v)	30	0.042
(vi)	45	0.041
(vii)	60	0.040

V.4.2.3. Effect of amount of APM

25 ml of 10^{-5} M MB dye solution having pH = 5.0±0.1 was taken in five beakers and a definite amount of APM was added to each of the beakers. The solutions were stirred for 5 minutes and centrifuged. From UV- Visible spectroscopy (Figure V.5) it was evident that the maximum removal efficiency (i.e. 94.6%) was obtained within 5 minutes of stirring when 25 ml of 10^{-5} M MB dye solution was treated with 0.125 g of APM.
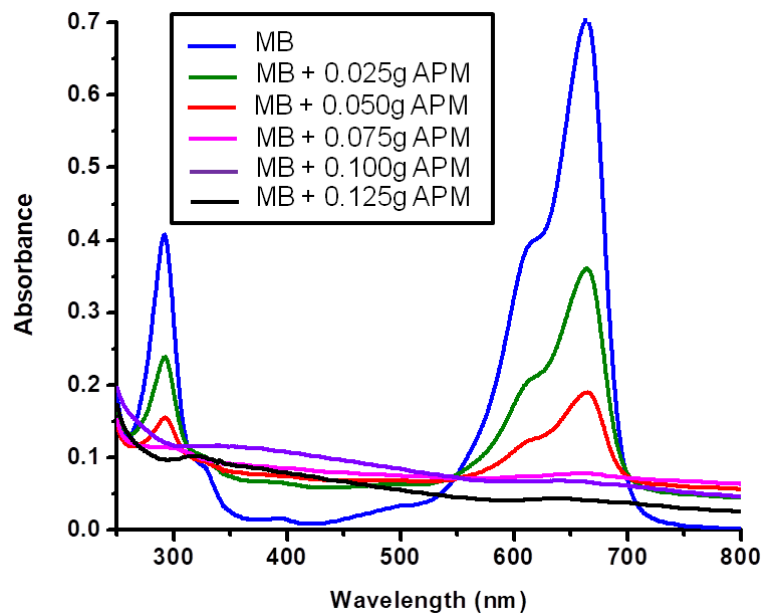
Figure V.5. Figure showing the decrease in intensity of absorbance peak of MB solution (λ_{max} = 660 nm) upon increasing the amount of APM.

V.4.2.4. Effect of nature of dye

In order to investigate the nature of dye, four different dyes *viz*. MB, EY, MG and MR were selected. 25 ml of 10^{-5} M solution of each dye (having pH = 5.0±0.1) was treated with 0.125 g of APM. The solutions were stirred for 5 minutes and centrifuged. In all the cases, the filtrate was analyzed using UV-Visible spectroscopy. The spectra indicated that MB, MR and MG had been removed from dye-contaminated water upon treatment with APM. The absence of absorbance peak between 650-700 nm, 500-550 nm and 600-650 nm respectively confirmed the removal of dye-stuffs from water (Figure V.6). However, in the case of EY there was no significant change in the absorbance peak before and after treatment with APM. The result suggested that APM was effective only for the removal of cationic dyes from water.
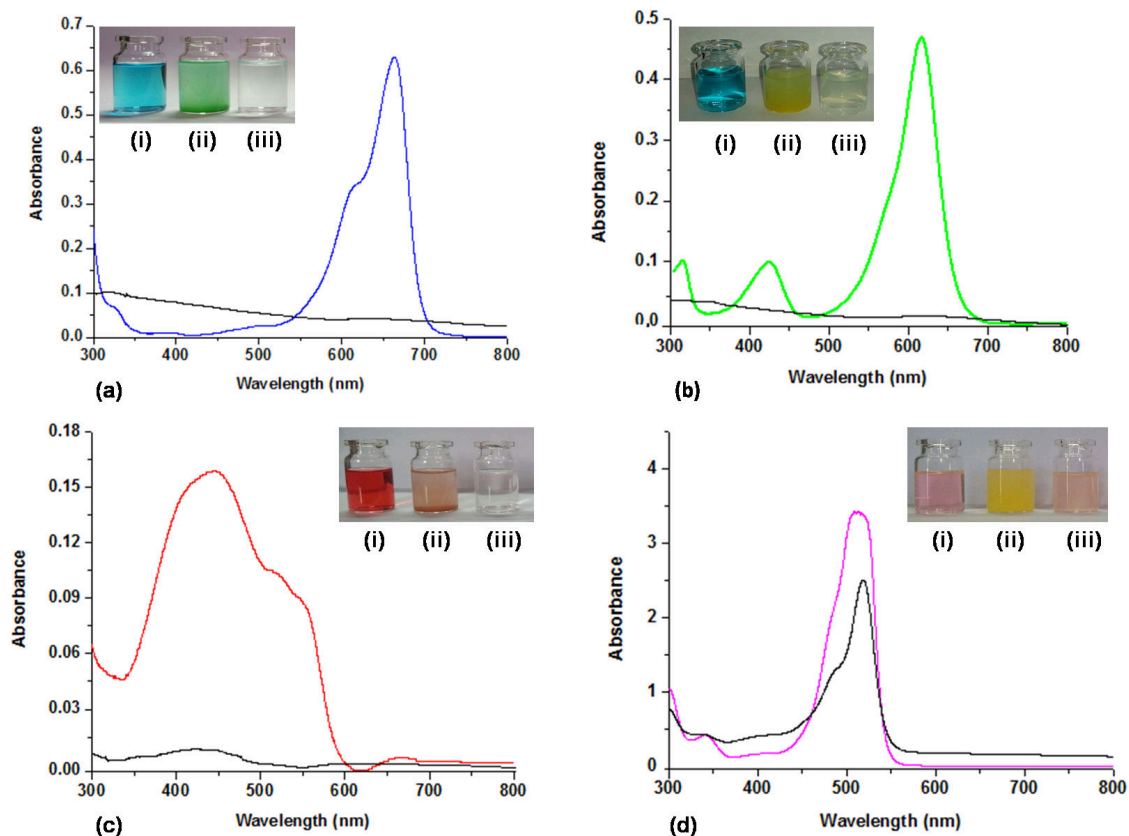
159

Figure V.6. UV-Visible spectra of 25 ml of 10^{-5} M dye solution having pH = 5.0±0.1 of (a) MB (b) MG (c) MR and (d) EY before (coloured curve) and after (black curve) treatment with 0.125 g of APM. Figure in the inset shows (i) original dye solution (ii) dye solution immediately after adding 0.125 g of APM (iii) filtrate of Bottle ii immediately after 5 minutes of stirring.

V.4.2.5. Influence of pH

25 ml each of 10^{-5} M MR, MG and MB solution was taken and its pH was adjusted between 1.0±0.1 to 6±0.1 using 1M HCl. The resultant dye solutions were treated with 0.125 g of APM. The investigations revealed that APM could effectively remove MB and MG from dye-contaminated water in the pH range 1-6. This could be attributed to the catioinic nature of MB and MG in the pH rage 1-6 (refer Figure V.7a and 7b). However, APM could not remove MR from solution at pH above 5 (refer Figure V.7c). A preview of literature suggested that MR exists as anionic dye at pH above 5 [42]. A similar result was obtained in the case of EY. EY exists either as a neutral or an anionic dye in the pH range 1-6 [43]. Therefore, there was no significant change in its absorbance peak before and after treatment with APM. The results suggested that perhaps ion-exchange of ammonium ions in APM with cationic dye moieties is responsible for the removal of dye-stuffs.

V.4.2.6. Reusability of APM

The reusability of APM for the removal of MB was analyzed for 20 cycles using 25 ml of 10^{-5} M dye solution having pH = 5.0±0.1. In the first cycle, 0.125 g of APM was added to MB solution, stirred for 5 minutes and centrifuged. APM thus obtained was air-dried and subsequently treated with 25 ml of 10^{-5} M dye solution having pH = 5.0±0.1 and this process was repeated for 20 cycles. The removal of MB was observed upto 16th cycles (Table V.4) wherein 94.6% removal efficiency was achieved. However, the contact time required to remove MB from dye-contaminated water increased with subsequent number of cycles. While only 5 minutes of stirring was required upto 4th cycle, 10 minutes of stirring was

required upto 8th cycle to achieve the removal efficiency of 94.6%. Therefore, the time of stirring was gradually increased 5 minutes per four cycles.
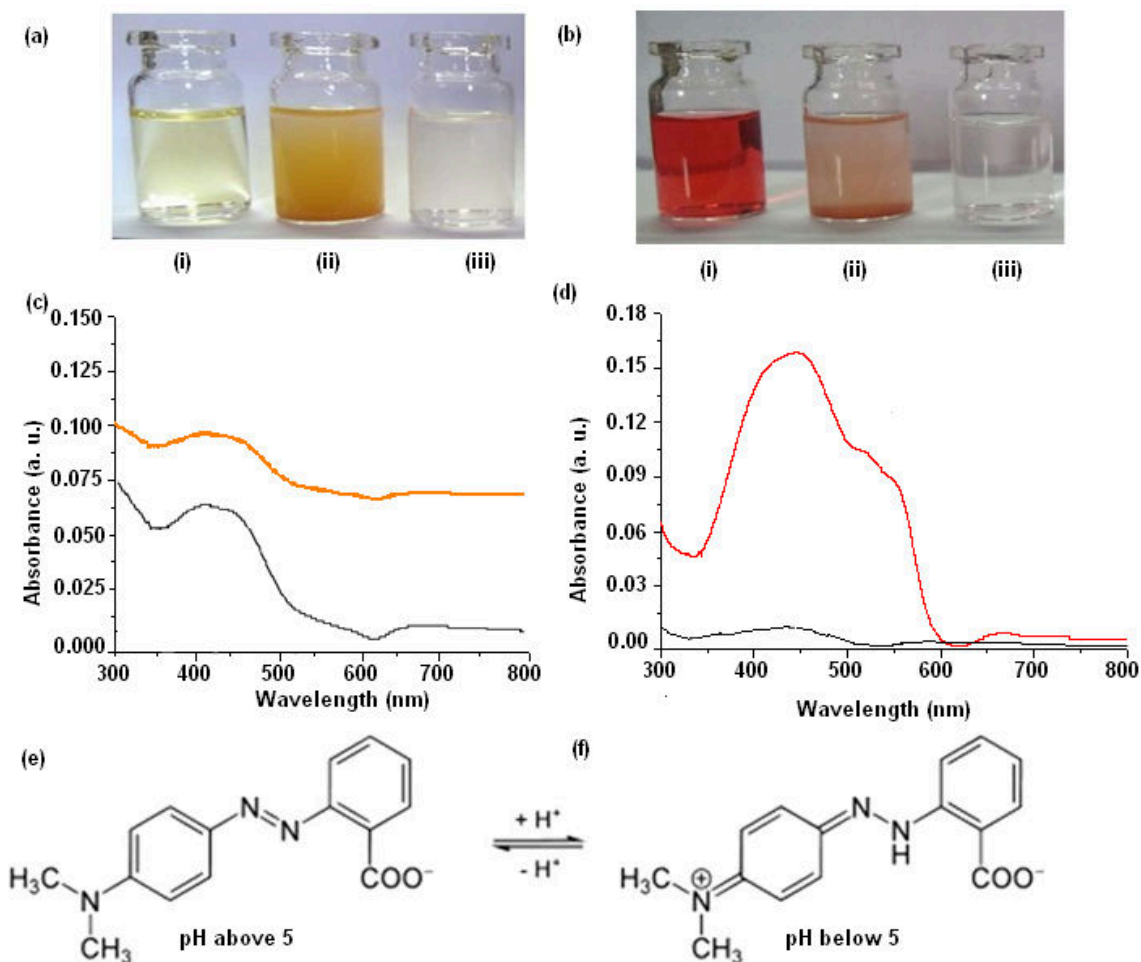

Figure V.7. (a) and (b) Dye solutions of MR at pH above and below 5 respectively with (i) original dye solution (ii) dye solution immediately after adding 0.125 g of APM (iii) filtrate of bottle (ii) immediately after 5 minutes of stirring. (c) and (d) UV-Visible spectra of dye solutions (i) and (iii) of MR shown in Figure 7a and 7b respectively. (e) and (f) Structure of MR at pH above and below 5 respectively.

Table V.4. Absorbance of MB solution upon treatment with APM at 660 nm after each cycle.

Number of cycles	Absorbance
Upto 16	0.041
17th	0.152
18th	0.343
19th	0.480
20th	0.650

V.4.2.7. Adsorption capacity of APM

The adsorption/desorption isotherm of APM, resembles that of Brunauer's Type I isotherm, that is the characteristic for microporous adsorbents (Figure V.8) [50]. The microporosity was confirmed from the mean pore diameter of 1.8158 nm obtained from Brunauer–Emmett-Teller (BET) plot. Further, the total pore volume of APM was estimated to confirm whether dye moieties could be adsorbed in the micro pores of APM. It was observed that pore volume had reduced from 8.013 x 10^{-2} to 3.0306 x 10^{-2} cm^3/g after APM had been treated with MB solutions for 16 cycles. The decrease in total pore volume confirmed the presence of MB moieties in the micropores of APM (refer Table V.5 for textural parameters of APM before and after the treatment of dye-stuffs).

Table V.5. Textural parameters of APM before (I) and after (II) the treatment of dye-stuffs.

Sl. No.	Textural parameter	I	II
1	Total pore volume (p/p^o=0.990) [cm^3/g]	8.0131 x 10^{-2}	3.0306 x 10^{-2}
2	Surface area (BET) [m^2/g]	1.7652 x 10^2	44.512
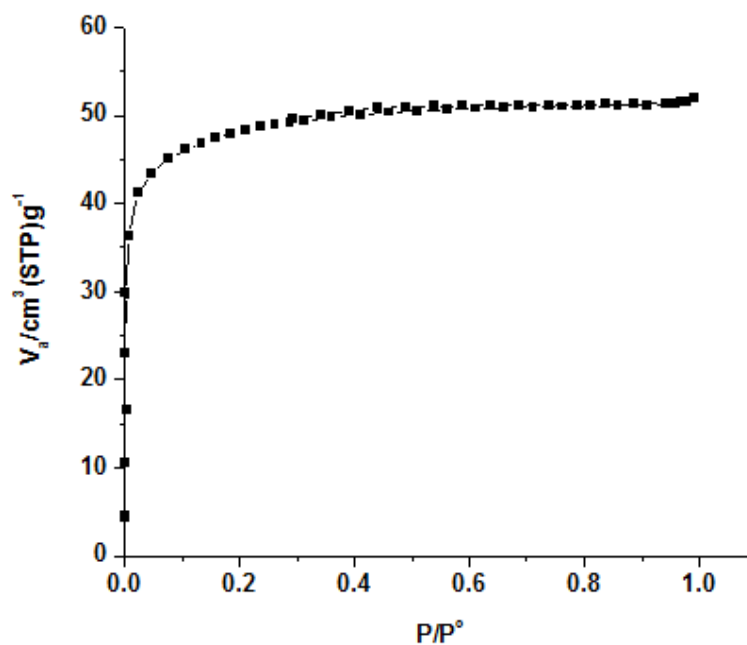
Figure V.8. The adsorption/desorption isotherm of APM which resembles that of Brunauer's Type I isotherm.

V.4.2.8. Mechanism

Based on the above observations it was evident that the presence of NH_4^+ ions in APM facilitates ion-exchange between NH_4^+ ions and cationic dye moieties. A preview of literature suggests that APM is an excellent adsorbent and it can adsorb metal ions such as Cs^+, K^+, Na^+, Sn^{2+}, Bi^{3+} etc. via ion-exchange between NH_4^+ ions and metal ions [51-53].

164

Therefore, a similar mechanism has been proposed herein. The removal of cationic dye-stuffs may be visualized as an ion-exchange process between NH_4^+ ions and cationic dye moieties (Figure V.9). It was confirmed by comparing the PXRD pattern of APM obtained after 16 cycles of treatment with MB with as-synthesized APM. A comparison of PXRD pattern indicated that APM maintains the cubic phase during the ion-exchange process between NH_4^+ ions and cationic dye moieties (Figure V.10). Further, sensitivity to pH enabled APM to reverse the cation exchange process.
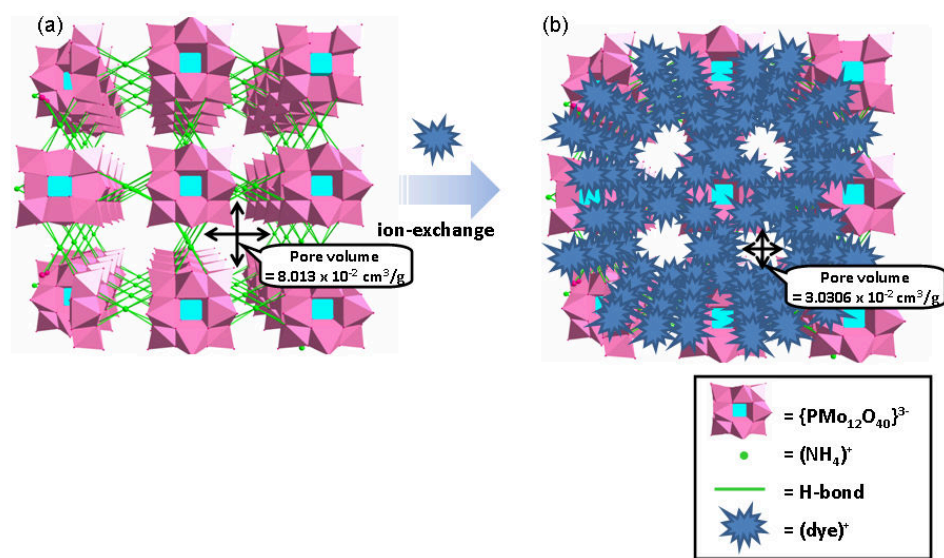

Figure V.9. (a) Crystal structure of APM. The lattice water molecules have been omitted for clarity. (b) Ion-exchange between NH_4^+ ions and cationic dye moieties.
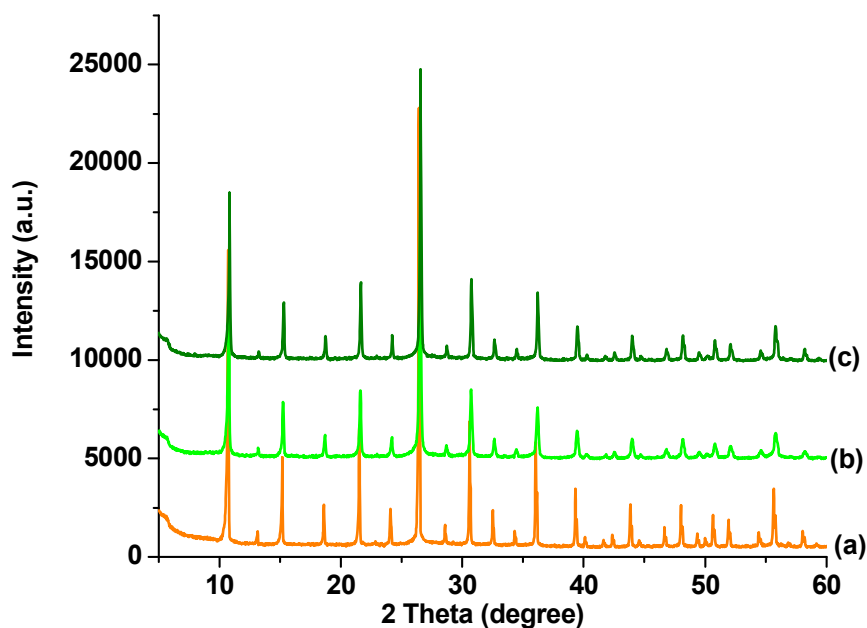
Figure V.10. Figure showing the PXRD pattern of (a) as-synthesized APM (b) APM obtained after 1st cycle of treatment with MB solution (c) APM obtained after 16th cycle of treatment with MB solution.

APM is stable only in acidic medium (pH $\leq$ 6) [14]. At pH $>$ 6, it disintegrates into its soluble molecular precursors i.e. NH_4^+, $\{PO_4\}^{3-}$ and $\{Mo_xO_y\}^{z-}$ ions [54]. Therefore, the present investigation was carried out at pH $\leq$ 6. At pH = 1–6, cationic dyes readily replace NH_4^+ ions in APM to form $\{Dye\}_3[PMo_{12}O_{40}]$. Interestingly, the ion-exchanged dye moieties could be regenerated in solution when APM was treated with 10 ml of 1 M NH_4Cl and 0.5 ml of NH_3 (Figure V. 10). However, the addition of NH_4Cl/NH_3 solution increased the pH of the medium (pH $>$ 7) and two outcomes are observed.

(a) In the case of MR, at pH $>$ 7 a clear yellow solution (**V**, refer Figure V.11a) was observed due to disintegration of APM and change in color of MR into yellow. Upon adjusting the pH of the solution **V** using 1 M HCl i.e. at pH = 5–6, APM and MR could be regenerated and separated by centrifugation and filtration.

(b) In the case of MB and MG, at pH > 7 {Dye}$_3$[PMo$_{12}$O$_{40}$] disintegrates into its soluble molecular precursors i.e. Dye, {PO$_4$}$^{3-}$ and {Mo$_x$O$_y$}$^{z-}$ moieties resulting in a clear blue solution **V** (refer Figure V.11b). However, upon addition of 1 M HCl, pH of the solution was adjusted between 1 and 6 wherein APM and dye could be regenerated as {Dye}$_3$[PMo$_{12}$O$_{40}$] i.e. residue **IV**.
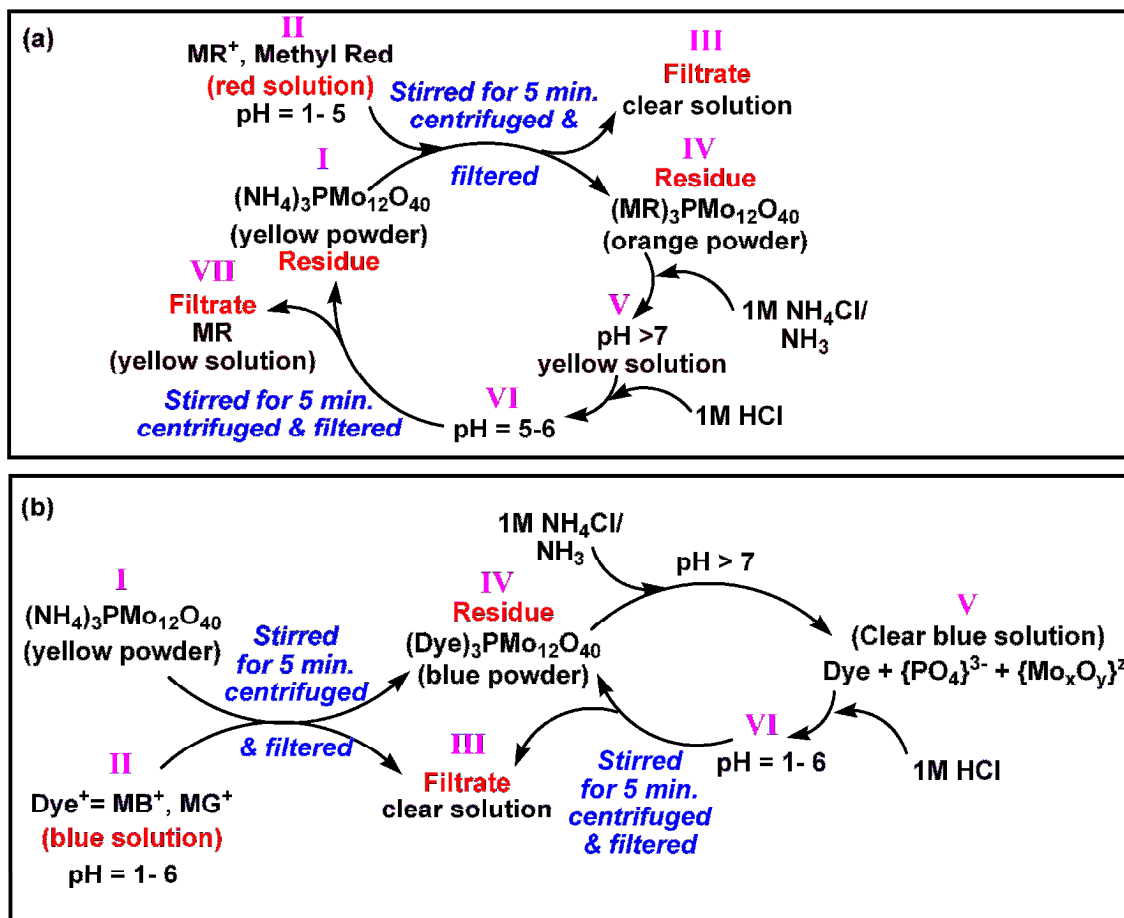

Figure V.11. Release of ion-exchanged dye moieties in solution upon treatment with 1M NH$_4$Cl and NH$_3$ solution. (a) Ion-exchange mechanism for MR. (b) Ion-exchange mechanism for MB and MG.

V.5. Conclusions

Micro-sized ammonium phosphomolybdate, $\{NH_4\}_3[PMo_{12}O_{40}].6H_2O$ particles were synthesized under ambient conditions and characterized. APM was found to be an effective medium for the removal of cationic dyes in acidic medium. While Methylene Blue and Malachite Green could be eliminated from dye-contaminated water in the pH range 1-6; Methyl Red could be removed only in the pH range 1-5. Dye removal efficiency as high as 94.6% was achieved upon treating 10^{-5} M MB solution (pH = 5.0±0.1) with APM. APM could be successfully re-used upto 16 cycles. The removal of dye-stuffs from contaminated water could be attributed to ion-exchange between ammonium ions in APM with cationic dye moieties. The ion-exchange process was found to be reversible which enabled APM and dye moieties to be regenerated in solution.

References

1. Parker, A. *Nature* **1932**, 130, 761-763.

2. Huang, Z.; Li, Y.; Chen, W.; Shi, J.; Zhang, N.; Wang, X.; Li, Z.; Gao, L.; Zhang, Y. *Mater. Chem. Phys.* **2017**, 202, 266-276.

3. Malarvizhi, R.; Ho, Y. S. *Desalination* **2010**, 264, 97-101.

4. Katheresan, V.; Kansedo, J.; Lau, S. Y. *J. Environ. Chem. Eng.* **2016**, 6, 4676-4697.

5. Tian, X.; Hou, L.; Wang, J.; Xin, X.; Zhang, H.; Ma, Y.; Wang, Y.; Zhang, Li.; Han, Z. *Dalton Trans*. **2018**, 47, 15121-15130.

6. Ali, I.; Peng, C.; Naz, I.; Lin, D.; Saroj, D. P.; Ali, M. *RSC Adv*. **2019**, 9, 3625-3646.

7. Khan, M. I.; Akhtar, S.; Zafar, S.; Shaheen, A.; Khan, M. A.; Luque, R.; Rehman, A. *Materials* **2015**, 8, 4147-4161.

8. Ahmad, A.; Setaper, S. H. M.; Chuo, S. C.; Khatoon, A.; Wani, W. A.; Kumar, R.; Rafatullah, M. *RSC Adv*. **2015**, 5, 30801-30818.

9. Erdemoglu, S.; Aksu, S. K.; Sayilkan, F.; Izgi, B.; Asilturk, M.; Sayilkan, H.; Frimmel, F.; Gucer, S. *J. Hazard. Mater*. **2008**, 155, 469-476.

10. Liu, L.; Lin, Y.; Liu, Y.; Zhu, H.; He, Q. *J. Chem. Eng. Data* **2013**, 58, 2248-2253.

11. Gupta, V. K.; Mittal, A.; Gajbe, V.; Mittal, J. *Ind. Eng. Chem. Res*. **2006**, 45, 1446-1453.

12. Wang, S.; Li, H.; Xu, L. *J. Colloid Interface Sci.* **2006**, 295, 71-78.

13. Kausar, A.; Iqbal, M.; Javed, A.; Aftab, K.; Nazli, Z.; Bhatti, H. N.; Noureen, S. *J. Mol. Liq*. **2018**, 256, 395-407.

14. Thomas, J.; Ramanan, *A. Cryst. Growth Des*. **2008**, 8, 3390-3400.

15. Thomas, J.; Ramanan, A. *Inorg. Chim. Acta* **2011**, 372, 243-249.

16. Thomas, J.; Kumar, D.; Ramanan, A. *Inorg. Chim. Acta* **2013**, 396, 126-135.

17. J. Thomas, Ph.D. Thesis, Indian Institute of Technology Delhi, India, **2010**.

18. Pathan, S.; Patel, A. *Catal. Sci. Technol*. **2014**, 4 648-656.

19. Wang, X.; Wang, J.; Geng, Z.; Qian, Z.; Han, Z. *Dalton Trans*. **2017**, 46, 7917-7925.

20. Gong, K.; Liu, Y.; Han, Z. *RSC Adv*. **2015**, 5, 47004-47009.

21. Ai, L.; Wang, Z.; He, F.; Wu, Q. *RSC Adv*. **2018**, 8, 34116-34120.

22. Pinto, T. V.; Fernandes, D. M.; Pereira, C.; Guedes, A.; Blanco, G.; Pintado, J. M.; Pereira, M. F. R.; Freire, C. *Dalton Trans*. **2015**, 44, 4582-4593.

23. Wang, J.; Shi, W.; Li, S.; Mao, Q.; Ma, P.; Niu, J. *Dalton Trans*. **2018**, 47, 7949-7955.

24. Sun, P.; Zhang, S.; Xiang, Z.; Zhao, T.; Sun, D.; Zhang, G.; Chen, M.; Guo, K.; Xin, X, *J. Coll. Inter. Sci*. **2019**, 547, 60-68.

25. Gong, Y.; Bai, F.; Yu, Z.; Bi, Y.; Xu, W.; Yu, L. *RSC Adv*. **2016**, 6, 8601-8604.

26. Clemente-Juan, J. M.; Coronado, E.; Gaita-Arino, A. *Chem. Soc. Rev*. **2012**, 41, 7464-7478.

27. Hu, G.; Dong, Y.; He, X.; Miao, H.; Zhou, S.; Xu, Y. *Inog. Chem. Commun*. **2015**, 60, 33-36.

28. Liu, C. G.; Guan, W.; Song, P.; Su, Z. M.; Yao, C.; Wang, E. B. *Inorg. Chem* **2009**, 48, 8115-8119.

29. Moll, H. E.; Zhu, W.; Oldfield, E.; Rodriguez-Albelo, L. M.; Mialane, P.; Marrot, J.; Vila, N.; Mbomekalle, I. M.; Riviere, E.; Duboc, C.; Dolbecq, A. *Inorg. Chem*. **2012**, 51, 7921-7931.

30. Qu, X.; Feng, H.; Ma, C.; Yang, Y.; Yu, X. *Inorg. Chem. Commun*. **2017**, 81, 22-26.

31. Berzelius, J. J. *Annalen der physic* **1826**, 83, 261-288.

32. Pandey, S. D.; Tripathi, P. *Electrochim. Acta* **1982**, 27, 1715-1721.

33. Basu, M.; Sarkar, S.; Pande, S.; Jana, S.; Sinha, A. K.; Sarkar, S.; Pradhan, M.; Pal, A.; Pal, T. *Chem. Commun*. **2009**, 7191-7193.

34. Gregg, S. J.; Stock, R. *Trans. Faraday Soc*. **1957**, 53, 1355-1362.

35. Sharma, S.; Sharma, M. K.; Chaturvedi, N. *Int. J. Chem. Res*. **2011**, 2, 20-22.

36. Sachdeva, D.; Parashar, B.; Bharadwaj, S.; Panjabi, P. B.; Sharma, V. K. *Int. J. Chem. Sci*. **2010**, 8, 1321-1328.

37. (a) Sharma, S.; Chaturvedi, N.; Chaturvedi, R. K.; Sharma, M. K. *J. Ind. Pollut. Control* **2010**, 26, 165-169.

   (b) Jakar, S.; Chaturvedi, R.; Sharma, M. K. *Int. J. Chem. Sci.* **2014**,12, 573-582.

38. Sharma, S.; Chaturvedi, N.; Chaturvedi, R. K.; Sharma, M. K. *Int. J. Chem. Sci*. **2010**, 8, 1580-1590.

39. Sharma, S.; Chaturvedi, N.; Chaturvedi, R. K.; Sharma, M. K. *Pollut. Res*. **2011**, 30, 165-168.

40. Bansal, A.; Sharma, D.; Ameta, R.; Sharma, H. S. *Int. J. Chem. Sci*. **2010**, 8, 2747-2755.

41. Joshi, A.; Vaidhya, S.; Singh, M. *J. Chem. Sci*. **2019**, 131, 1-7.

42. Ayed, L.; Mahdhi, A.; Cheref, A.; Bakhrouf, A. *Desalination* **2011**, 274, 272-277.

43. Sharma, N.; Jha, R.; Baghel, S.; Sharma, D. *J. Alloy. Comp*. **2017**, 695, 270-279.

44. Chauhan, N.; Singh, V.; Kumar, S.; Kumari, M.; Sirohi, K. *J. Mol. Struct*. **2019**, 1185, 219-228.

45. Abbassi, R.; Yadava, A. K.; Kumar, N.; Huanga, S.; Jaffea, P. R. *Ecol. Eng*. **2013**, 61, 366-370.

46. Qi, M.; Yu, K.; Su, Z.; Wang, C.; Wang, C.; Zhou, B.; Zhu, C. *Inorg. Chim. Acta* **2013**, 400, 59-66.

47. Tadjarodi, A.; Zad, A. I.; Imani, M. *Mater. Lett*. **2015**, 161, 464-467.

48. Ilhan, S.; Kahruman, C.; Yusufoglu, I. *J. Anal. Appl. Pyrolysis* **2007**, 78, 363-370.

49. Dermeche, L.; Thouvenot, R.; Hocine, S.; Rabia, C. *Inorg. Chim. Acta* **2009**, 362, 3896-3900.

50. Lowell S.; Shields J. E. *Adsorption isotherms. In: Powder Surface Area and Porosity*; Springer, Dordrecht **1984**, 11-13.

51. Abu-Zied, B. M.; Farrang, A. A.; Asiri, A. M. *Powder Tech*. **2013**, 246, 643-649.

52. Smit, J. V. R. *Nature* **1958**, 181, 1530-1531.

53. Park, Y.; Shin, W. S.; Choi, S. J. *Chem. Eng. J*. **2013**, 220, 204-213.

54. Alcaniz-Monge, J.; Trautwein, G.; Roman-Martinez, M. C. *Solid State Sci*. **2011**, 13, 30-37.